特约专栏

Research on Materials and Superconductivity in Iron Pnictides

WEN Haihu
(National Laboratory for Superconductivity, Institute of Physics,
Chinese Academy of Sciences, Beijing 100190, China)

Abstract: The discovery of superconductivity at 26 K in F doped LaOFeAs has stimulated enormous interests in the field of condensed matter physics. In short two years more than 1 000 scientific papers have been published, the family of the iron pnictide superconductors has been quickly expanded to seven different structures and the superconducting transition temperature has been rapidly raised to about 55 ~ 57 K. In additional the pairing mechanism has been categorized as unconventional with the antiferromagnetic spin fluctuations probably as the pairing media. This article will give a brief review on the progress of both materials and physics in this field. We will also give some perspectives on the possible applications of these new superconductors.

Key words: iron based superconductors; novel superconductivity; pairing mechanisms; antiferromagnetism; spin fluctuations

CLC number: O511$^+$.3 Document code: A Article ID: 1674 - 3962(2010)08 - 0018 - 09

铁磷族化合物及其超导电性

闻海虎
(中国科学院物理所 国家超导实验室, 北京 100190)

摘 要: 氟掺杂的 LaFeAsO 中 26 K 超导电性的发现极大地促进了凝聚态物理的发展。在短短的两年时间中, 已经有过千篇文章发表, 已经有七种新结构被发现, 超导转变温度也被迅速提升到了 55 ~ 57 K。此外, 在 超导机理方面这类化合物也已经被认定属于非常规, 而反铁磁自旋涨落被认为是导致超导配对的媒介。从材料和物理学的角度对这类化合物的性质和超导机理给出了简单的综述。还对未来的研究及应用给出了一些展望。

关键词: 离子基超导体; 新超导电性; 配对机制; 反铁磁性; 自旋涨落

1 Introduction

Superconductivity is achieved by the quantum condensation of large amount of paired electrons in the condensed matter. The consequence of this condensation is the vanishing of resistivity at finite temperatures and exclusion of magnetic field. Due to the excellent performance of a superconductor under a high current or magnetic field, any new superconductors with high transition temperatures are highly desired, for the purpose of potential applications. By the end of February 2008, a Japanese group led by Hosono in Tokyo Institute of Technology, found superconductivity at 26 K in F doped LaOFeAs[1]. This type of materials can be traced back to 1974 when Jeitschko et al. were exploring the new functional materials[2]. Later on, a German group fabricated a lot of materials with the same ZrCuSiAs structure[3]. They are generally called as quaternary oxypnictides in a general formula as *Ln*O*MPn* (where *Ln* = La, Ce, Pr, Nd, Sm; Eu and Gd, etc.; *M* = Mn, Fe, Co and Ni, etc.; *Pn* = P and As, etc.). In Fig. 1 we show the typical structure for LaOFeAs. The system has a layered structure and a tetragonal P4/nmm space group, with a stacking series of $-(LnO)_2-(MP)_2-(LnO)_2-$ along c-axis. In one unit cell, there are two molecules of *Ln*O*MP*, and it is valence self-balanced in the parent phase, i. e., $(LnO)^{+1}$ is balanced by $(MP)^{-1}$. Some of them, the Fe and Ni based compounds, were shown to be superconductors and thus constructed another new family of superconductors without copper[4-5].

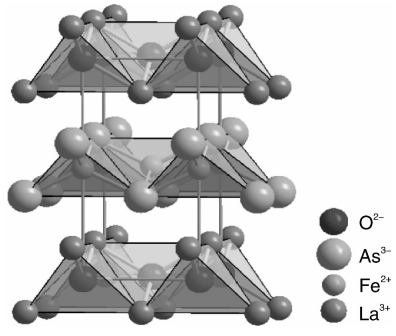

Fig. 1 Skeleton of the LaFeAsO structure. The LaO and FeAs layers stack along *c*-axis alternatively

Received date: 2010 - 08 - 16
Foundation item: 973 National Program(2006CB601000, 2006CB921802)
Biography: Wen Haihu, Professor

2 Materials and structures

The discovery of superconductivity at 26 K in F-doped LaFeAsO has stimulated a new round of intense study in the field of superconductivity. Since then, the chasing of fabricating the new iron pnictide superconductors has been taken in a dramatic way. Within short two years, about seven different structures of the FeAs family members have been found. In Figure 2, we present the chart plot of the seven different structures of FeAs-based materials found so far. Just by their formulas, they are called in short now as 11, 111, 122, 1111, 32522 and 21311 (or 42622), and the latest 43822. It is evident that all the families have the FeAs planes as the basic building layers, and they are sandwiched by other layers which are supposed to be the charge donors, or making the internal pressure so as to influence the electronic properties. In Table 1, we also give the transition temperatures and the lattice parameters of all the structures. So far, only the 32522 family does not exhibit clear evidence of superconductivity, all other families show superconductivity with the highest transition temperatures (55 ~ 57 K) in the 1111 family[6-8].

Table 1　Six different structures and typical superconductors in the FeAs based system (*RE* = rare earth, *AE* = alkaline earth, *TM* = 3 d - 5 d transition metals)

Families	Formula	T_c	Lattice parameters a, c/nm As height to Fe-plane h/nm	Bond angles/(°) $\alpha_{Fe-As-Fe}$　$\beta_{As-Fe-As}$
11	$Fe_{1+x}Se$, $FeTe_{1-x}Se_x$ FeSe or FeTe (HP)	8 K[9] 27 K[10-11]	$a=0.3792$, $c=0.5955$ $h=0.1617$	$\alpha=99.08$ $\beta=114.9°$
111	LiFeAs	13 K[12]	For LiFeAs $a=0.3791$, $c=0.6364$, $h=0.1505$	$\alpha=103.1$ $\beta=112.74$
	NaFeAs	13 K[13]	For NaFeAs $a=0.3945$, $c=0.6997$, $h=0.1416$	$\alpha=108.65$ $\beta=109.88$
1111 Oxygen based	Electron doping: $REFeAsO_{1-x}F_x$ Hole doping: $RE_{1-x}AE_xFeAsO$	55 ~ 56 K[6,8,14,15] 25 K[16,17]	$NdFeAsO_{1-x}F_x$ $a=0.3985$, $c=0.8622$, $h=0.1333$	$\alpha=112.43$ $\beta=108.01$
1111 Fluorine based	$AE_{1-x}RE_xFeAsF$ (*RE* = rare earth, *AE* = Ba, Sr, Ca)	56 ~ 57 K[18,7,19]	CaFeAsF $a=0.3993$, $c=0.8955$, $h=0.1367$	$\alpha=111.2$ $\beta=108.61$
122	$AE_{1-x}AL_xFe_2As_2$ $AE(Fe_{1-x}TM_x)_2As_2$ $AEFe_2As_{2-x}P_x$	38 K[20] 20 ~ 28 K[21-24] 30 K[25-26]	$BaFe_2As_2$ $a=0.3917$, $c=1.3297$, $h=0.1380$	$\alpha=109.66$ $\beta=109.38$
32522	$Sr_3Sc_2O_5Fe_2As_2$	0 K[27]	$a=0.4069$, $c=2.6876$, $h=0.1338$	$\alpha=113.34$ $\beta=107.57$
21311(42622)	Sr_2VO_3FeAs	37 K[28] 46 K (HP)[29] HP = high pressure	$a=0.3930$, $c=1.5673$, $h=0.1425$	$\alpha=108.1$ $\beta=110.16$
43822	$Ca_4(Mg,Ti)_3O_{8-\delta}Fe_2As_2$	42 K[30]	$a=0.3877$, $c=3.337$, $h=0.14$	$\alpha=108.33$ $\beta=110.05$

In the FeAs-based superconductors, the Fe-layer is formed in a square lattice structure with the Fe-Fe distance of about 0.26 nm. The As atoms reside on top and below the Fe-layer alternatively and locate at the center of the Fe-atom squares. Three typical bond angles are marked by α, β and γ, as shown in Figure 2 and 3. The four As atoms and one Fe atom construct a tetrahedron. These bond angles, together with the height between the As to the Fe-planes are essential in governing the superconductivity as argued by Lee et al.[31] and Kuroki et al.[32]. Empirically it was found that the highest superconducting transition temperature occurs with a regular tetrahedron, $\alpha=\beta=109°$, $\gamma=71°$, but the underlying physics is still unknown. Actually the As-Fe height dependence of T_c is also non-monotonic function[33].

The band structure calculation was done on the LaFePO system in 2007[34]. In the FeAs system, the band structure looks quite similar to that in the LaFePO system: the five orbits of the Fe-3d electrons, i. e., xy, x^2-y^2, xz, yz, $3z^2-r^2$ all cross

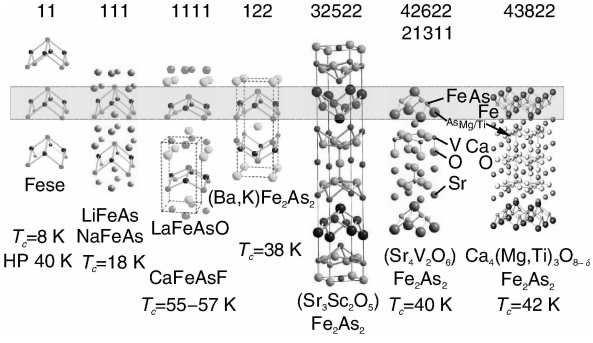

Fig. 2　Seven different structures of the FeAs-based materials which contain the FeAs planes as marked by the frame. The formulas given here represent the typical ones. *RE* stands for the rare earth elements

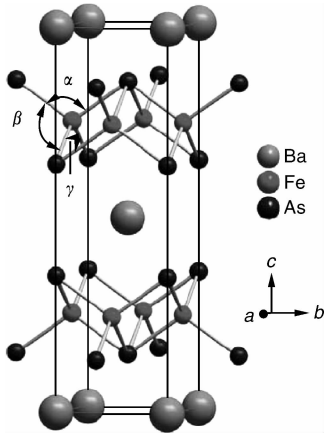

Fig. 3 The skeleton plot of the atomic structure of $BaFe_2As_2$. Three typical bond angles α, β and γ are marked here

the Fermi energy yielding a complicated Fermi surfaces (FS)[35]: three sets of hole like FSs locating around Γ-Z, while other two sets with roughly cylindrical shapes around M-A. Since there are two Fe atoms in one unit cell, therefore the two electron FSs in the Brillouin zone are actually folded, leading to two sets of crossing elliptic FSs around the M-A as shown in Fig. 4.

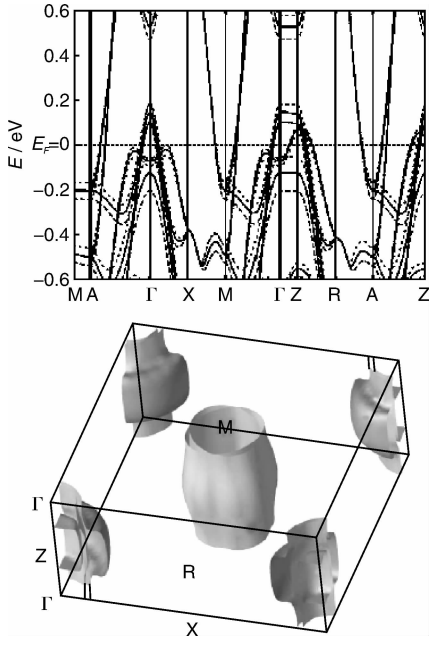

Fig. 4 (left) Band structures of the five orbits of LaFeAsO based the local spin density approximation (LSDA) and the generalized gradient approximation (GGA) by Singh and Du. (Right) Five sets of Fermi surfaces derived from the calculation. Note that the three sets of hole like FSs locate at the corner (Γ-point) and the two sets of electron-like FSs at the center (M-point)

3 Understandings on the superconducting mechanism

3.1 Abandoning of phonon mechanisms

The first assessment on the phonon mediated pairing was made by Boeri et al.[36]. It was found that the electron-phonon coupling constant is quite small: $\lambda_{e\text{-}ph} = 0.21$, in the LaFeAsO system. Taking a Debye temperature of about 300 K[37] and using the standard Migdal-Eliashberg theory, this gives a maximum T_c of 0.8 K. This is certainly far below the T_c value measured. The updated calculation on the effect of local magnetic moments on the electron-phonon coupling in $BaFe_2As_2$ using the density functional perturbation theory finds an enhanced electron-phonon coupling constant $\lambda_{e\text{-}ph} = 0.35$, but it is still not enough to explain the high critical temperature[38]. Although some preliminary isotope effect points to a relationship $T_cM^\alpha = \text{const}$ with $\alpha = 0.33$ to 0.5[39], while the repeated experiments in the same system $Ba_{0.6}K_{0.4}Fe_2As_2$ showed an opposite results: the exponent α is small and negative[40]. This may suggest that the atomic mass, although involved in a subtle way in influencing the superconducting transition temperature, should not be the dominant factor. As we will see below that in the picture of AF spin fluctuation mediated pairing mechanism, the mass of the iron is indeed only a trivial factor which should not give any definite, even qualitative indication about the mass isotope effect. Of course, we are not clear yet how strong effect would be given by the spin-orbital interaction and/or phonon-magnetic interaction. In terms of the AF spin fluctuation mediated pairing, the phonons may play as the pair breakers. Clearly, more experiments from different groups on the isotope effect are desired to clarify whether the phonon pairing mechanism can be totally abandoned.

3.2 Original proposals for S ±

With the quite good nesting condition between the hole and electron pockets, it is natural to think that the electronic system will response significantly with the AF spin fluctuations, especially when the AF vector matches nicely with the interpocket displacement. This interesting picture was first proposed by Mazin et al.[41], and later on further formalized by several other groups based on different theoretical approaches[42-44]. More details about the pairing order parameter can be found in the recent review[45]. The basic idea is illustrated in Figure 5, where the two

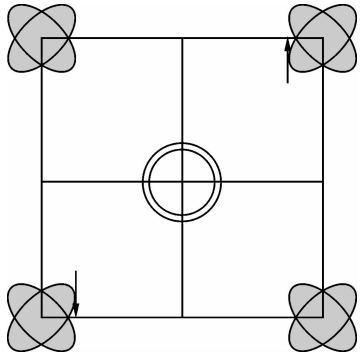

Fig. 5 Cartoon picture about the Fermi surfaces and the interpocket electron scattering. The two electrons on the electron pockets marked by the two arrows, will be scattered to the hole pockets as marked by the red circles in the center of the Brillouin Zone, and vice versa

electrons on the electron (hole) FSs marked with the thick arrows with opposite directions of spins, will be scattered to the hole (electron) FSs by exchanging the AF spin fluctuations. If the pairing is really established through exchanging the AF spin fluctuation, it is electronic in origin and to avoid the strong repulsive interaction is actually the driving force for pairing[46]. According to the Eliashberg equation as shown in Eq. (1),

$$\Delta(k) = -\sum V(k,k')\frac{\Delta(k')}{2E(k')}\tanh\left(\frac{1}{2}\beta E(k')\right) \qquad (1)$$

a positive interaction $V(k, k')$, like exchanging the AF spin fluctuations, would lead to a sign change of the order parameter $\Delta(k)$ and $\Delta(k')$ if k and k' reside on the hole and elec-

tron pockets. Therefore an extended s-wave gap, with opposite signs on the hole and the electron FSs are understandable. This kind of s-wave gap has been supported by part experiment already, while the direct evidence is still lacking. Perhaps the resonance observed in the inelastic neutron scattering and the recent scanning tunneling (STM) spectroscopy measurements in the $FeTe_{1-x}Se_x$ samples give more direct evidence for this kind of unique pairing[47]. We shall address this point in next section.

3.3 Phase diagram and the roles played by mutiband effect and AF spin fluctuations

In most of these structures(11, 1111, 122), the material starts with showing an antiferromagnetic state in the stoichiometric undoped case[48]. By doping either electrons or holes, the antiferromagnetic order will be suppressed and the superconductivity will emerge. Taking the 122 phase as the example, we show two phase diagrams in Figure. 6 by doping holes in $Ba_{1-x}K_xFe_2As_2$ system and doping electrons in $Ba(Fe_{1-x}Co_x)2As_2$. The first impression about the phase diagram of iron pnictide superconductors is that it looks quite similar to that of the cuprate superconductors. Indeed both systems start with the antiferromagnetic (AF) order as the parent phase. The superconductivity is achieved by suppression this AF order. In addition, in both systems, holes and electrons can be doped into the functioning layers, CuO planes in the cuprates and FeAs planes in the iron pnictides, leading to the systematic evolution of magnetism and superconductivity. However, further studies revealed some differences between them.

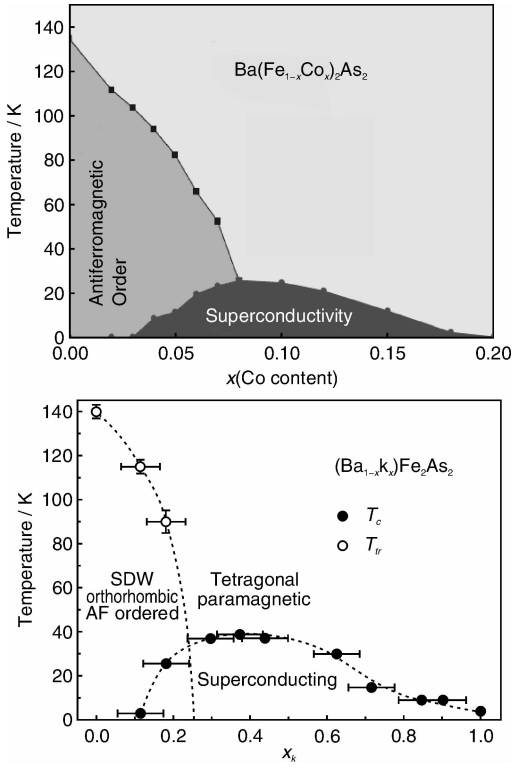

Fig. 6　Typical phase diagrams of the iron pnictide superconductors based on the (right) $Ba_{1-x}K_xFe_2As_2$ and (left) $Ba(Fe_{1-x}Co_x)_2As_2$ systems

Firstly, the superconducting dome is actually asymmetric in the iron pnictide superconductors, but quite symmetric in the cuprates. The T_c ramps up quickly in the underdoped side, but decays in a slow rate in the overdoped region. Based on the measurements and analysis of Hall effect and resistivity, Fang et al.[49] gave a natural explanation of this asymmetric doping dependence. In Figure 7, we show the temperature and doping

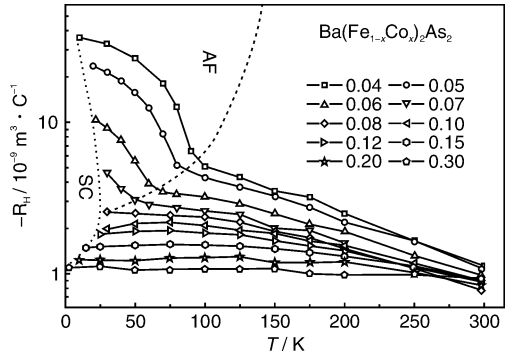

Fig. 7　The temperature dependence of the Hall coefficient R_H at 9 T. The red dashed line at $x < 0.07$ follows T_{AF} below which R_H rises sharply, indicating a dramatic change of the carrier concentration and scattering rate, as discussed in the text. The blue dotted line outlines the superconducting region

dependence of the Hall coefficient R_H in wide doping regime. One can see that, below T_{AF} in the underdoped side, the Hall coefficient R_H increases drastically. This can be understood as the sharp drop of the DOS as well as the scattering rate (especially the electron band) due to the formation of the long range AF order. Therefore we can say that the superconductivity and the AF order are competing for density of states in the underdoped side, and the superconducting transition temperature is getting lower towards more underdoping. While in the overdoped region, the AF spin fluctuation, which is assumed as the major media for the pairing, is getting weaker, therefore the T_c decreases slowly. This can be supported by the gradual vanishing of the temperature dependence of R_H. In a single band system, the Hall coefficient R_H should depend weakly on temperature assuming the magnetic scattering is weak, while in the multiband case, the R_H can be strongly temperature dependent due to the involvement of scattering rates from different bands. For example, in the case of two bands, the Hall coefficient R_H can be written as

where $\sigma_i = \dfrac{e^2 n_i \tau_i}{m^i}$ with n_i, m_i and τ_i the charge carrier density,

$$R_H = \frac{\sum (\sigma_i^2 / n_i^H)}{\sum \sigma_i^2} \tag{2}$$

effective mass and relaxation time of the i^{th} band. Actually in very clean MgB_2 films, we also observed a strong temperature dependence of the Hall coefficient R_H[50], which can be understood very well in the same picture. Actually this scenario can also get the support from the NMR measurements which show that the spin relaxation rate $1/T_1T$ diverges when approaching the AF ordering temperature T_{AF} (see Figure 8). The $1/T_1T$ measures the q integral of the imaginary part of the dynamical spin susceptibility in the Brillouin zone, therefore $1/T_1T$ reflects the summation of all different q modes of spin fluctuations[51]. This strong temperature dependence of $1/T_1T$ above T_{AF} is attributed to the AF-SF. Once this "enhancement" or "divergence" vanishes, or AF-SF becomes very weak, the superconductivity also disappears. Combining the Hall effect and the NMR data $1/T_1T$, we can clearly see the importance of both the multiband effect and AF spin fluctuations for superconductivity. These experiments give support to the pairing model by exchanging the AF-SF as the pairing media.

The second difference between the iron pnictide and cuprates is that the superconductivity in the former can be induced

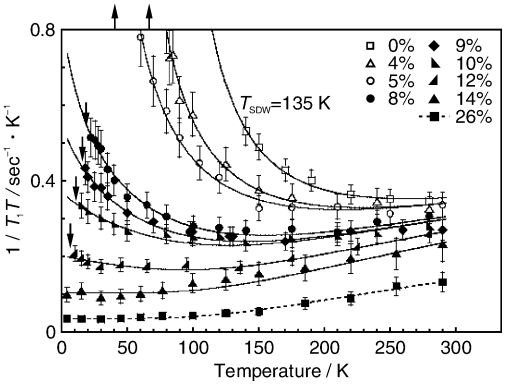

Fig. 8 The $1/T_1T$ measured at As(0) sites for various concentrations x with magnetic field B applied along the ab plane. Solid and dashed arrows mark T_c and T_{AF}, respectively. Solid and dashed curves are the best fits with (for $x \leqslant 0.14$) and without (for $x \geqslant 0.26$) a Curie-Weiss term arising from AF-SF.

by the pressure effect and even isovalence chemical doping to the parent phase, this has actually not been observed in the cuprates. In Figure. 9 we show the pressure induced and the isovalence doping induced superconductivity[52-54]. It is clear that, not only charge doping, but also structural parameters give significant influence to the electronic properties and thus alter the superconductivity.

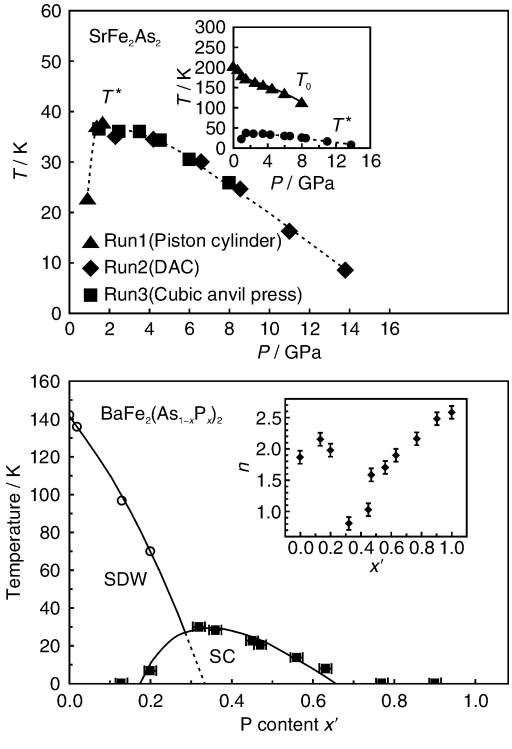

Fig. 9 Pressure and isovalence chemical doping induced superconductivity. (left) The phase diagram under pressure in $SrFe_2As_2$. (right) The phase diagram in the isovalence doping system $BaFe_2(As_{1-x}P_x)_2$

3.4 Experimental progress on the pairing symmetries

Superconductivity is achieved by the condensation of the paired electrons, therefore the symmetry of the pairing function, or the order parameter is very essential to identify the mechanism of superconductivity. For several members of the family of Fe-based superconductors the NMR data have positively identified the parity of the superconducting state as singlet[55-56] essentially leaving only two possibilities for the angular momentum of the Cooper pairs: $L=0$ (s-wave) and $L=2$ (d-wave). In the following we will give a brief review of the experimental progress about the pairing symmetry of the superconducting gaps. We will not describe it in different techniques, rather in different families 122, 1111 and 11, in which the pairing symmetry have been intensively studied. Thus we can have a deeper insight of the pairing symmetry together with the different structures.

3.4.1 122 family

We start with the experimental data in the 122, since single crystals with large size and quite good qualities can be obtained with this family. The early experiment on the $Ba_{1-x}K_xFe_2As_2$ family was given by Ding et al. using ARPES[57]. Isotropic gaps were found on the hole pockets around Γ-FSs. The gap of the inner Γ-FS (α) is about 12 meV and that on the outer Γ-FS (β) is about 6 meV. The measurements on the more arguable electron pockets M-FS (γ) at some high symmetric points tell also isotropic gap with the value of about 12 meV. Similar conclusion was also drawn from another group[58]. Cautions must be taken, however, that the energy- distributive- curves (EDC) of ARPES normally do not show a well resolved coherent peak associating with the long life quasiparticles in the superconducting state (besides that from the inner hole pocket, the α-FS defined in Ref. [57]). It is important to note that the gaps were derived from the shallow "coherent peaks" after the symmetrization, not from the leading-edge shift. This may lead to some uncertainties in drawing the final conclusion, especially on the electron pocket (γ-FS). In addition, according to the five orbital calculations, the gap feature is clearly k_z dependent[59]. This indicates that further refined ARPES measurements would be necessary to resolve the 3D FSs and the gap symmetry on them. According to the theory, the nodes may be well expected at somewhere of the FSs.

The specific heat measurements shown in Figure10 on the similar sample $Ba_{1-x}K_xFe_2As_2$ indicate at least two components, with the dominant one of a full gap and the gap energy of about 6 meV (as shown in Fig. 10)[60]. An enhancement of the electronic specific heat coefficient $\gamma_e(T)$ in the intermediate temperature region may be explained as the second component with a small gap or nodes on the energy gap[59]. The roughly linear, but with slight curvature of the magnetic field dependence of the electronic specific coefficient also support this statement. This conclusion is also supported by the thermal conductivity measurements in a slightly underdoped sample[61]. A very small thermal conductivitycoefficient $k_0/T = 5\ \mu W/K^2 \cdot cm$ (see Figure 11) was measured at $T \to 0$ K, which is much smaller than the estimated value ($140\ \mu W/K^2 \cdot cm$) if there would be a line node (as shown in Fig. 11)[61]. However, the clear field dependence of k_0/T in the low field region indicates a gap minimum somewhere. This analysis suggests a small gap which may have a value of about 1 ~ 2 meV. This result is in contrast with the earlier ARPES data which suggest the smaller gap of about 6 meV. Actually, multigap feature with the smaller gap in the scale of 1 ~ 4 meV was evidenced by the measurements of $H_{c1}(T)$. By measuring the lower critical field, Ren et al.[62] derived the two gaps: $\Delta_s \sim 2$ meV, and $\Delta_l \sim 9$ meV. Recalling the ARPES data, the gap is large if one defines the gap from the position of the coherent peak, while the gap could be much smaller if it is determined from theleading-edge shift of the EDC. Actually, the measurements of superfluid density using the tunnel diode resonator (TDR) technique find a decrease of the penetration depth as $1/\lambda^2 \propto 1-(T/T_c)^n$ with $n=2 \sim 2.5$ (see Figure 12)[63-64]. For

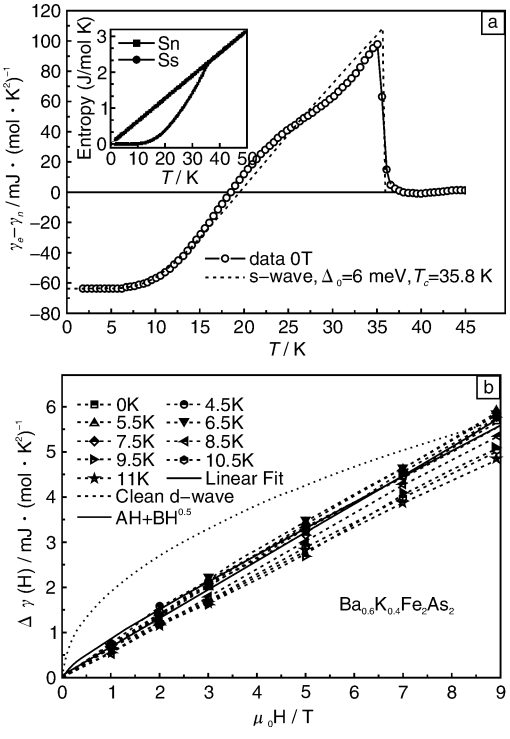

Fig. 10　(a) Temperature dependence of the electronic SH contribution $\gamma(T)$ with the normal-state part subtracted in $Ba_{0.6}K_{0.4}Fe_2As_2$. A sharp SH anomaly with $\Delta C/T|_{T_c}$ can be seen here. A hump is clearly seen in the intermediate temperature region. The red dashed line is a theoretical curve based on the BCS expression with an s-wave gap of 6 meV. The inset shows the entropy of the superconducting state red circle symbols and the normal state by dark square symbols. (b) Field dependence of the field-induced SH $\Delta\gamma(H)$. The blue solid, red dotted, and navy-blue solid line are the linear fit to the zero-temperature data, the fit to the *d*-wave prediction $\Delta\gamma(H) = AH^{1/2}$, and the fit by mixing the above two components, respectively

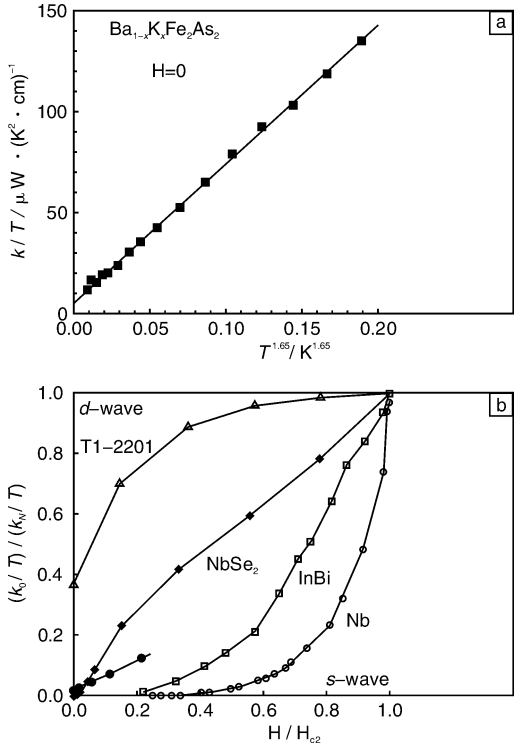

Fig. 11　(left) Temperature dependence of the thermal conductivity of the underdoped $Ba_{1-x}K_xFe_2As_2$ single crystal with T_c = 28 K. The residual value of k_0/T is very small compared with the one estimated from the d-wave model. (right): comparison of the magnetic field dependence of k_0/T for the $Ba_{1-x}K_xFe_2As_2$ single crystal and other superconducting samples. The results can be understood with a full gap but one of the gap value is very small.

a superconductor with line nodes and impurity scattering in the unitary limit, the superfluid density indeed decreases with T^2. An alternative way, as adopted by the authors, is to explain the this power law relation as contributions of multiband superconductivity with the S ± pairing gap and presence of impurity scattering[65]. It is interesting to note that the universal exponent $n = 2 \sim 2.5$ found here in many different kind of samples with different impurity scales, may not be easily described by the model. The data may suggest some kind of nodes in the sample, as we shall address below.

In the 122 family, a system with accumulated evidence of nodes is the phosphor doped $BaFe_2As_2$[66]. It was supposed that this kind of doping will only change the internal pressure and thus give influence on the chemical potential, therefore it was called as the isovalence doping. The evidence of line nodes comes from the penetration depth measurements which shows a clear linear temperature dependence in the $T=0$ limit[66]. A non-linear field dependence, being close to a square-root relation, of the thermal conductivity k_0/T was also observed[66], which adds more evidence for a line node in this particular system. But interestingly, the field dependence of the specific heat was found to be linear[67], which was attributed to the fact that the specific heat is specially detecting the heavier but fully gapped Γ-FS. These contrasting results on thermal conductivity and specific heat are clearly needed to be reconciled with a more general picture. Recently, the penetration depth measurements with the inducting field along the FeAs planes, thus the inducting current flows along both the *ab*- and *c*-axes, was conducted and the results show that the temperature dependence of the penetration depth is still describable by the power law $1/\lambda^2 \propto 1 - (T/T_c)^n$, while with a smaller exponent $n = 1 \sim 1.5$[68]. This indicates that there might be nodal features along the *z*-axis. Thermal conductivity measured with thermal current along *ab*-plane and *c*-axis indeed show the

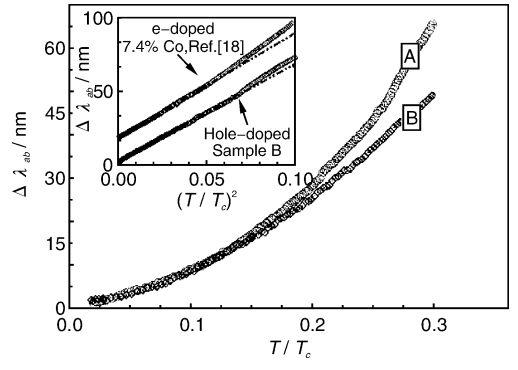

Fig. 12　The temperature dependence of the penetration depth, both the hole doped (K-doping) and electron doped (electron doping) give the relation $1/\lambda^2 \propto 1 - (T/T_c)^n$ with n close to 2. It is interesting that this kind of power law seems to be a general feature of the 122 system in either doping the electrons and holes

sharp difference[69]. This result is by no means in contradicting with the earlier conclusion of the thermal conductivity, since the in plane thermal transport needs the finite value of the in-plane Fermi velocity. One possible way to understand this dilemma is that the line nodes may exist at somewhere of the Fermi surface where the perpendicular Fermi velocity v_F^c is dominant, while the parallel Fermi velocity v_F^{ab} is very small. With the extremely warped Fermi surface detected by the quantum oscillation[70], this picture is valid if we assume a horizontal line node on the disc like 3D Fermi surface.

3.4.2 1111 system

In the 1111 system, the most notable experiment about the gap symmetry was made on the LaFePO sample. The penetration depth measurements from two groups show the linear temperature dependence in the limit of $T \to 0$[70-71]. This kind of linear decrease of the superfluid density with temperature is quite difficult to be understood within a full-gap model. The presence of line nodes in LaFePO was explained as the results of the pairing of multi-orbital effect[58]. It was suggested that the individual orbit has different weights in different part of the Fermi pockets. Therefore the pairing interaction has also angle dependence along individual Fermi pocket, the node may appear at the joint point of two orbitals. For the LaFePO system, the calculation indicates the presence of nodes[31,58], giving support to the experimental observation.

The results about pairing symmetry in other families of the 1111 phase, mainly the FeAs-based materials, remain highly controversial. For example, the penetration depth measurements in F-doped PrFeAsO[71] and SmFeAsO[72] reveal the existence of two full gaps, where the μSR measurements indicate the nodal gap feature or a small gap[73]. The local magnetic mapping measurements found no simultaneously generated half vortices, suggesting that weak links in high pressure synthesized NdFeAsO-F samples have predominantly 0 phase shifts or non-existence of the nodal gap[74], while in the similar samples, the "phase sensitive" measurements found the trace of half vortices[75]. All these contradicting results call for further refined experiments in large and high quality single crystals in this family.

3.4.3 11 system

The 11 system was found to be superconductive at about 8 K in the material $Fe_{1+x}Se$[9]. The transition temperature was improved to about 37 K under pressure in FeTe system or the $FeTe_{1-x}Se_x$ systems[10-11]. The experiments done for the pairing symmetry in this family are quite few. NMR measurements on the single crystal $Fe_{1.04}Te_{0.67}Se_{0.33}$ found that the spin relaxation rate $1/T_1 \propto T^3$[76], which should be proportional to TN_F^2 with the N_F the DOS at E_F. This relationship together with the finite residual DOS in the $T = 0$ K limit were attributed to the presence of the line nodes in the superconducting gap. However, this conclusion is not supported by the in-plane thermal conductivity measurements. As in all other FeAs-based superconductors, Dong et al. found a very small value of the residual thermal conductivity coefficient k_0/T obtained in the in-plane thermal transport measurements. The authors further found that the field dependence k_0/T of in $FeSe_x$ ($T_c = 8.8$ K) exhibits a feature very similar to the 2H-NbSe, in which multigaps with the smallest one of about 0.5 meV were found by ARPES[77]. Therefore in the $FeTe_{1-x}Se_x$ system, either a very small gap or an highly anisotropic gap among the multigaps is anticipated. The STM spectrum measured at 0.4 K shows also a full gap feature[47]. The remarkable point of this STM work is to find the "sign-flips" of the quasiparticle scattering interference pattern with zero and finite magnetic fields. These results are explained as the evidence of the S ± pairing manner. While, we should notice that, even with a full gap feature seen by the STM, this does not mean that the nodes on other FSs are also absent, since sometime STM measurements depend strongly on the tunneling matrix element effect. Therefore, in the iron pnictide superconductors, one cannot conclude the absence of nodes if one does not see it. However, if one can see it, that normally means the presence of nodes. In recent experiments of angle dependence of low temperature specific heat, Zeng et al.[78] observed a four fold oscillation. This is attributed to the anisotropic of the gaps and the gap minimum appears at the two folded electron Fermi pockets, i. e., along the Fe-Fe bond. Clearly there are still a lot of uncertainties about the gap structure in the 11 system.

4 Perspectives and concluding remarks

Clearly the iron-based new superconductors provide a new platform for the research of superconductivity, probably unconventional in nature. The high upper critical field, relatively small anisotropy and larger coherence length (compared to the cuprate superconductors) make the materials very encouraging for applications. From the presented data we know already that the critical fields are much larger than that of MgB_2. Concerning the mechanism, it is highly desired to know whether the AF order is a common feature for all systems in the undoped case, obviously the AF spin fluctuation has a close relationship with superconductivity. From the experimental data obtained up to now, it seems possible that the s-wave wave pairing gap with opposite signs exist on the electron and hole pockets. More refined data from single crystals will clarify all these and to illustrate how the Fermi surface looks like and how does it evolve with the doping.

5 Concluding remarks

(1) So far, seven different structures of the FeAs-based materials have been synthesized, they are named by the formulas as 11, 111, 122, 1111, 32522, 21311, 43822 all containing the unique FeAs-layers. The superconductivity with the highest transition temperature 55 ~ 57 K, occurs in the 1111 system. It was suggested that both the bond angle Fe-As-Fe and the height of As to the Fe planes are essential to the superconductivity. These two factors will give nontrivial influence on the electronic structures and consequently on superconductivity.

(2) Most of the systems start with an antiferromagnetic order as the parent phase. The superconductivity is induced by either charge doping, pressure effect or the isovalence doping. Hall effect and NMR measurements show the importance of multiband effect and antiferromagnetic spin fluctuations to superconductivity.

(3) In addition to the original proposal for the pairing via exchanging the antiferromagnetic spin fluctuation, theoretically five orbital calculations were done leading to the natural expectation of nodes, or nodal s-wave gap on some part of Fermi surfaces.

(4) The experiments about the pairing symmetry remain highly controversial. The unique pairing manner, i. e., the sign reversing of the pairing order parameters on the hole and electron pockets, is still recalling for more evidence, especially direct evidence. While it is clear that, nodes may exist on the gap at some part of the Fermi surfaces, both be inferred from the theoretical calculations or some experiments. The resonance observed in the inelastic neutron scattering and the recent STM data on the $FeTe_{1-x}Se_x$ samples, if interpreted correctly, may be understood as the direct evidence for the pairing with the sign reversed order parameter.

6 ACKNOWLEDGMENTS

I would like to acknowledge Bin Zeng, Xiyu Zhu, Bing

Shen, Peng Cheng in helping to make this manuscript. This work is supported by the projects from MOST of China, NSFC and CAS. Part of the content of this review paper will appear as well in the Annual Reviews (A Nonprofit Scientific Publisher).

References

[1] Kamihara Y, Watanabe T, Hirano M, *et al.* Iron-Based Layered Superconductor La[$O_{1-x}F_x$]FeAs ($x = 0.05 \sim 0.12$) with $T_c = 26$ K[J]. *J Am Chem Soc*, 2008, 130: 3 296 – 3 297.

[2] Johnson V, Jeitschko W. ZrCuSiAs: A "Filled" PbFCl Type[J]. *J Solid State Chem*, 1974, 11: 161 – 166.

[3] Zimmer B I, Jeitschko W, Albering J H, *et al.* The Rate Earth Transition Metal Phosphide Oxides LnFePO, LnRuPO and LnCoPO with ZrCuSiAs Type Structure[J]. *J Alloys and Comp*, 1995, 229: 238 – 242.

[4] Kamihara Y, Hiramatsu H, Hirano M, *et al.* Iron-Based Layered Superconductor: LaOFeP[J]. *J Am Chem Soc*, 2006, 128: 10 012 – 10 013.

[5] Watanabe T, Yanagi H, Kamiya T, *et al.* Nickel-Based Oxyphosphide Superconductor with a Layered Crystal Structure, LaNiOP [J]. *Inorg Chem*, 2007, 46: 7 719 – 7 721.

[6] Ren Z A, Lu W, Yang J, *et al.* Superconductivity at 55 K in Iron-Based F-Doped Layered Quaternary Compound Sm[$O_{1-x}F_x$] FeAs[J]. *Chin Phys Lett*, 2008, 25: 2 215 – 2 216.

[7] Cheng P, Shen B, Mu G, *et al.* High-Tc Superconductivity Induced by Doping Rare-Earth Elements into CaFeAsF[J]. *Europhys Lett*, 2009, 85: 67 003.

[8] Wang C, Li L J, Chi S, *et al.* Thorium-Doping-Induced Superconductivity up to 56 K in $Gd_{1-x}Th_xFeAsO$[J]. *Europhys Lett*, 2008, 83: 67 006.

[9] Hsu F C, Luo J Y, Yeh K W, *et al.* Superconductivity in the PbO-Type Structure α-FeSe[J]. *PNAS*, 2008, 105: 14 262 – 14 264.

[10] Mizuguchi Y, Tomioka F, Tsuda S, *et al.* Superconductivity at 27 K in Tetragonal FeSe under High Pressure[J]. *Appl Phys Lett*, 2008, 93: 152 505.

[11] Imai T, Ahilan K, Ning F L, *et al.* Why Does Undoped FeSe Become a High-T_c Superconductor under Pressure[J]. *Phys Rev Lett*, 2009, 102: 177 005.

[12] Wang X C, Liu Q Q, Lv Y X, *et al.* The Superconductivity at 18 K in LiFeAs System[J]. *Solid State Commun*, 2009, 148: 538 – 540.

[13] Tapp J H, Tang Z J, Lv B, *et al.* LiFeAs: An intrinsic FeAs-based superconductor with $T_c = 18$ K[J]. *Phys Rev B*, 2008, 78: 060505(R).

[14] Chen X H, Wu T, Wu G, *et al.* Superconductivity at 43 K in $SmFeAsO_{1-x}F_x$[J]. *Nature*, 2008, 453: 761 – 762.

[15] Kito H, Eisaki H, Iyo A. Superconductivity at 54 K in F-Free $NdFeAsO_{1-y}$[J]. *J Phys Soc Jpn*, 2008, 77: 063 707.

[16] Wen H H, Mu G, Fang L, *et al.* Superconductivity at 25 K in Hole-Doped ($La_{1-x}Sr_x$)OfeAs[J]. *Europhys Lett*, 2008, 82: 17 009.

[17] Mu G, Zeng B, Zhu X Y, *et al.* Synthesis, Structural, and Transport Properties of the Hole-Doped Superconductor $Pr_{1-x}Sr_xFeAsO$[J]. *Phys Rev B*, 2008, 79: 104 501.

[18] Zhu X Y, Han F, Cheng P, *et al.* Superconductivity in Fluoride-Arsenide $Sr_{1-x}La_xFeAsF$ Compounds[J]. *Europhys Lett*, 2009, 85: 17 011.

[19] Wu G, Xie Y L, Chen H, *et al.* Superconductivity at 56 K in Samarium-Doped SrFeAsF[J]. *J Phys: Cond Mat*, 2009, 21: 142 203.

[20] Rotter M, Tegel M, Johrendt D. Superconductivity at 38 K in the Iron Arsenide ($Ba_{1-x}K_x$)Fe_2As_2[J]. *Phys Rev Lett*, 2008, 101: 107 006.

[21] Sefat A S, Huq A, McGuire M A, *et al.* Superconductivity in $LaFe_{1-x}Co_xAsO$[J]. *Phys Rev B*, 2008, 78: 104 505.

[22] Ni N, Tillman M E, Yan J Q, *et al.* Effects of Co Substitution on Thermodynamic and Transport Properties and anisotropic H_{c2} in $Ba(Fe_{1-x}Co_x)_2As_2$ Single Crystals[J]. *Phys Rev B*, 2008, 78: 214 515.

[23] Cao G H, Wang C, Zhu Z W, *et al.* Superconductivity Induced by Cobalt Doping in Iron-Based Oxyarsenides[J]. *Phys Rev B*, 2009, 79: 054 521.

[24] Han F, Zhu X Y, Cheng P, *et al.* Superconductivity and Phase Diagrams of the 4 d- and 5 d-Metal-Doped iron Arsenides $SrFe_{2-x}M_xAs_2$ (M = Rh, Ir, Pd)[J]. *Phys Rev B*, 2009, 80: 024 506.

[25] Ren Z, Tao Q, Jiang S, *et al.* Superconductivity Induced by Phosphorus Doping and Its Coexistence with Ferromagnetism in $Eu-Fe_2(As_{0.7}P_{0.3})_2$[J]. *Phys Rev Lett*, 2009, 102: 137 002.

[26] Kasahara S, Shibauchi K, Hashimoto K, *et al.* *Evolution from Non · Fermi to Fermi liquid Transport Properties by Isovalent in $BaFe_2(As_{1-x}P_x)_2$ Superconducters*[EB/OL]. [2010], arXiv: 0905, 4427.

[27] Zhu X Y, Han F, Mu G, *et al.* $Sr_3Sc_2Fe_2As_2O_5$ as a Possible Parent Compound for FeAs-based Superconductors[J]. *Phys Rev B*, 2009, 79: 024 516.

[28] Zhu X Y, Han F, Mu G, *et al.* Transition of Stoichiometric Sr_2VO_3FeAs to a Superconducting State at 37.2 K[J]. *Phys Rev B*, 2009, 79: 220 512(R).

[29] Kotegawa H, Kawazoe T, Tou H, *et al.* Contrasting Pressure Effects in $Sr_2VFeAsO_3$ and $Sr_2ScFePO_3$[J]. *J Phys Soc Jpn*, 2009, 78: 123 707.

[30] Ogino H, Shimizu Y, Ushiyama K, *et al.* Superconductivity Above 40 K Observed in a New Iron Arsenide Oxide (Fe_2As_2)(Ca_4(Mg, Ti)$_3O_y$)[J]. *Applied Physics Express* 3, 2010, 3: 063 103.

[31] Lee C H, Iyo A, Eisaki H, *et al.* Effect of Structural Parameters on Superconductivity in Fluorine-Free $LnFeAsO_{1-y}$(Ln = La, Nd)[J]. *J Phys Soc Jpn*, 2008, 77: 083 704.

[32] Kuroki K, Usui H, Onari S, *et al.* Pnictogen Height as a Possible Switch between High-T_c Nodeless and Low-T_c Nodal Pairings in the Iron-Based Superconductors[J]. *Phys Rev B*, 2009, 79: 224 511.

[33] Mizuguchi Y, Hara Y, Deguchi K, *et al.* Anion Height Dependence of T_c for the Fe-Based Superconductor[J]. *Supercond Sci Technol*, 2010, 23: 054 013.

[34] Lebegue S. Electronic Structure and Properties of the Fermi Surface of the Superconductor LaOFeP[J]. *Phys Rev B*, 2007, 75: 035 110.

[35] Singh D J, Du M H. Density Functional Study of $LaFeAsO_{1-x}F_x$: A Low Carrier Density Superconductor Near Itinerant Magnetism [J]. *Phys Rev Lett*, 2008, 100: 237 003.

[36] Boeri L, Dolgov O V, Golubov A A. Is $LaFeAsO_{1-x}F_x$ an Electron-Phonon Superconductor[J]. *Phy Rev Lett*, 2008, 101: 026 403.

[37] Mu G, Zhu X Y, Fang L, *et al.* Nodal Gap in Fe-Based Layered Superconductor $LaO_{0.9}F_{0.1-\delta}FeAs$ Probed by Specific Heat Measurements[J]. *Chin Phys Lett*, 2008, 25: 2 221 – 2 224.

[38] Boeri L, Calandra M, Mazin I I, *et al.* *Effects of Magnetism and Doping on the Electron-Phonon Coupling in $BaFe_2As_2$*[EB/OL]. arXiv: 1004. 1943.

[39] Liu R H, Wu T, Wu G, *et al.* A Large Iron Isotope Effect in $SmFeAsO_{1-x}F_x$ and $Ba_{1-x}K_xFe_2As_2$[J]. *Nature*, 2009, 459: 64 – 67.

[40] Shirage P M, Kihou K, Miyazawa K, *et al.* Inverse Iron Isotope Effect on the Transition Temperature of the (Ba, K)Fe_2As_2 Superconductor[J]. *Phys Rev Lett*, 2009, 103: 257 003.

[41] Mazin I I, Singh D J, Johannes M D, *et al.* Unconventional Superconductivity with a Sign Reversal in the Order Parameter of $LaFeAsO_{1-x}F_x$[J]. *Phys Rev Lett*, 2008, 101: 057 003.

[42] Kuroki K, Onari S, Arita R, *et al.* Unconventional Pairing Originating from the Disconnected Fermi Surfaces of Superconducting $LaFeAsO_{1-x}F_x$[J]. *Phys Rev Lett*, 2008, 101: 087 004.

[43] Wang F, Zhai H, Ran Y, *et al.* Functional Renormalization-Group Study of the Pairing Symmetry and Pairing Mechanism of the FeAs-Based High-Temperature Superconductor[J]. *Phys Rev*

Lett, 2009, 102: 047 005.
[44] Yao Z J, Li J X, Wang Z D. Spin Fluctuations, Interband Coupling and Unconventional Pairing in Iron-Based Superconductors [J]. *New J Phys*, 2009, 11: 025 009.
[45] Mazin I I. Superconductivity Gets an Iron Boost [J]. *Nature*, 2010, 464: 183 - 186.
[46] Scalapino D. *A Common Thread*[EB/OL]. *arXiv*: 1002. 2413.
[47] Hanaguri T, Niitaka S, Kuroki K, *et al*. Unconventional s-Wave Superconductivity in Fe(Se, Te) [J]. *Science*, 2010, 328: 474 - 476.
[48] De La Cruz C, Huang Q, Lynn J W, *et al*. Magnetic Order Close to Superconductivity in the Iron-Based Layered $LaO_{1-x}F_xFeAs$ Systems[J]. *Nature*, 2008, 453: 899 - 902.
[49] Fang L, Luo H Q, Cheng P, *et al*. Roles of Multiband Effects and Electron-Hole Asymmetry in the Superconductivity and Normal-State Properties of $Ba(Fe_{1-x}Co_x)_2As_2$ [J]. *Phys Rev B*, 2009, 80: 140 508(R).
[50] Yang H, Liu Y, Zhuang C G, *et al*. Fully Band-Resolved Scattering Rate in MgB_2 Revealed by the Nonlinear Hall Effect and Magnetoresistance Measurements[J]. *Phys Rev Lett*, 2008, 101: 067 001.
[51] Ning F L, Ahilan K, Imai T, *et al*. Contrasting Spin Dynamics between Underdoped and Overdoped $Ba(Fe_{1-x}Co_x)_2As_2$ [J]. *Phys Rev Lett*, 2010, 104: 037 001.
[52] Igawa K, Okada H, Takahashi H, *et al*. Pressure-Induced Superconductivity in Iron Pnictide Compound $SrFe_2As_2$ [J]. *J Phys Soc Jpn*, 2009, 78: 025 001.
[53] Kimber S A J, Kreyssig A, Zhang Y Z, *et al*. Similarities between Structural Distortions under Pressure and Chemical Doping in Superconducting $BaFe_2As_2$ [J]. *Nature Materials*, 2009, 8: 471 - 475.
[54] Jiang S, Xing H, Xuan G F, *et al*. Superconductivity up to 30 K in the Vicinity of the Quantum Critical Point in $BaFe_2(As_{1-x}P_x)_2$[J]. *J Phys: Condens Matte*, r, 2009, 21: 382 203.
[55] Matano K, Ren Z A, Dong X L, *et al*. Spin-Singlet Superconductivity with Multiple Gaps in $PrFeAsO_{0.89}F_{0.11}$ [J]. *Europhys Lett*, 2008, 83, 57 001.
[56] Nakai Y, Ishida K, Kamihara Y, *et al*. Evolution from Itinerant Antiferromagnet to Unconventional Superconductor with Fluorine Doping in $LaFeAs(O_{1-x}F_x)$ Revealed by ^{75}As and ^{139}La Nuclear Magnetic Resonance[J]. *J Phys Soc Jpn*, 2008, 77: 073 701.
[57] Ding H, Richard P, Nakayama K, *et al*. Observation of Fermi-Surface-Dependent Nodeless Superconducting Gaps in $Ba_{0.6}K_{0.4}Fe_2As_2$[J]. *Europhys Lett*, 2008, 83: 47 001.
[58] Zhao L, Liu H Y, Zhang W T, *et al*. Multiple Nodeless Superconducting Gaps in $(Ba_{0.6}K_{0.4})Fe_2As_2$ Superconductor from Angle-Resolved Photoemission Spectroscopy [J]. *Chin Phys Lett*, 2008, 25: 4 402 - 4 405.
[59] Graser S, Maier T A, Hirschfeld P J, *et al*. Near-Degeneracy of Several Pairing Channels in Multiorbital Models for the Fe Pnictides [J]. *New J Phys*, 2009, 11: 025 016.
[60] Mu G, Luo H Q, Wang Z S, *et al*. Low Temperature Specific Heat of the Hole-Doped $Ba_{0.6}K_{0.4}Fe_2As_2$ Single Crystals [J]. *Phys Rev B*, 2009, 79: 174 501.
[61] Luo X G, Tanatar M A, Reid J P, *et al*. Quasiparticle Heat Transport in Single-Crystalline $Ba_{1-x}K_xFe_2As_2$: Evidence for a k-Dependent Superconducting gap without Nodes[J]. *Phys Rev B*, 2009, 80: 140 503(R).
[62] Ren C, Wang Z S, Luo H Q, *et al*. Evidence for Two Energy Gaps in Superconducting $Ba_{0.6}K_{0.4}Fe_2As_2$ Single Crystals and the Breakdown of the Uemura Plot[J]. *Phys Rev Lett*, 2008, 101: 257 006.
[63] Gordon R T, Ni N, Martin C, *et al*. Unconventional London Penetration Depth in Single-Crystal $Ba(Fe_{0.93}Co_{0.07})_2As_2$ Superconductors[J]. *Phys Rev Lett*, 2009, 102: 127 004.
[64] Martin C, Gordon R T, Tanatar M A, *et al*. Nonexponential London Penetration Depth of External Magnetic Fields in Superconducting $Ba_{1-x}K_xFe_2As_2$ Single Crystals[J]. *Phys Rev B*, 2009, 80: 020 501(R).
[65] Bang Y, Choi H, Won H. Impurity effects on the ± s-wave state of the iron-based superconductors[J]. *Phys Rev B*, 2009, 79: 054 529.
[66] Nakai y, Ishida K, Matsuda Y, *et al*. *Anisotropic Superconducting Properties of Optimally Doped* $BaFe_2(As_{0.65}P_{0.35})_2$ *under Pressure*[EB/OL]. [2010]. arXiv: 1006, 5830vl.
[67] Kim J S, Hirschfeld P J, Stewart G R, *et al*. *Specific Heat vs Field in the* 30 *K Superconductor* $BaFe_2(As_{0.7}P_{0.3})_2$[EB/OL]. *arXiv*: 1002. 3355.
[68] Martin C, Kim H, Gordon R T, *et al*. Evidence from Anisotropic Penetration Depth for a Three-Dimensional Nodal Superconducting Gap in Single-Crystalline $Ba(Fe_{1-x}Ni_x)_2As_2$ [J]. *Phys Rev B*, 2010, 81: 060 505(R).
[69] Reid J P, Tanatar M A, Luo X G, *et al*. Nodes in the Gap Structure of the Iron Arsenide Superconductor $Ba(Fe_{1-x}Co_x)_2As_2$ from *C*-Axis Heat Transport Measurements [J]. *Phys Rev B*, 2010, 82: 064 501.
[70] Shishido H, Bangura A F, Coldea A I, *et al*. Evolution of the Fermi Surface of $BaFe_2(As_{1-x}P_x)_2$ on Entering the Superconducting Dome[J]. *Phys Rev Lett*, 2010, 104: 057 008.
[71] Hashimoto K, Shibauchi T, Kato T, *et al*. Microwave Penetration Depth and Quasiparticle Conductivity of $PrFeAsO_{1-y}$ Single Crystals: Evidence for a Full-Gap Superconductor[J]. *Phys Rev Lett*, 2009, 102: 017 002.
[72] Malone L, Fletcher J D, Serafin A, *et al*. Magnetic Penetration Depth of Single-Crystalline $SmFeAsO_{1-x}F_y$ [J]. *Phys Rev B*, 2009, 79: 140 501(R).
[73] Luetkens H, Klauss H H, Khasanov R, *et al*. Field and Temperature Dependence of the Superfluid Density in $LaFeAsO_{1-x}F_x$ Superconductors: A Muon Spin Relaxation Study[J]. *Phys Rev Lett*, 2008, 101: 097 009.
[74] Hicks C W, Lippman T M, Huber M E, *et al*. Limits on the Superconducting Order Parameter in $NdFeAsO_{1-x}F_y$ from Scanning SQUID Microscopy[J]. *J Phys Soc Jpn*, 2008, 78: 013 708.
[75] Chen C T, Tsuei C C, Ketchen M B, *et al*. Integer and Half-Integer Flux-Quantum Transitions in a Niobium-Iron Pnictide Loop [J]. *Nature Physic s*, 2010, 6: 260 - 264.
[76] Michioka C, Ohta H, Matsui M, *et al*. *Unconventional Superconductivity in the Novel Layered Superconductor Fe(Te-Se) Investigated by* ^{125}Te *NMR on the Single Crystal* [EB/OL]. *arXiv*: 0911. 3729.
[77] Yokoya T, Kiss T, Chainani T, *et al*. Fermi Surface Sheet-Dependent Superconductivity in 2H-$NbSe_2$ [J]. *Science*, 2001, 294: 2518 - 2520.
[78] Zeng B, Mu G, Luo H Q, *et al*. *Anisotropic Structure of the Order Parameter in* $FeSe_{0.4}Te_{0.6}$ *Revealed by Angle Resolved Specific Heat*[EB/OL]. *arXiv*: 1004. 2236.